

ture of Bi^+ and $[\text{Bi}_5]^{3+}$. With this fixed point and the spectrum of Bi^+ on a molar absorptivity scale, we calculated the absorbance of Bi^+ in the mixture at all wavelengths and subtracted the result from the total absorbance to get the absorbance of $[\text{Bi}_5]^{3+}$. Having determined the concentration of $[\text{Bi}_5]^{3+}$ in the mix-

ture, we converted absorbance to molar absorptivity. A spectrum calculated in this way is given in Figure 8.

Acknowledgment.—We record our thanks to Jorulf Brynstad, who repeatedly clarified our thinking during the course of this investigation.

CONTRIBUTION FROM THE METALS AND CERAMICS DIVISION,
OAK RIDGE NATIONAL LABORATORY, OAK RIDGE, TENNESSEE 37830

Ligand Field Theory of $p^{2,4}$ Configurations and Its Application to the Spectrum of Bi^+ in Molten Salt Media^{1a}

BY HAROLD L. DAVIS, NIELS J. BJERRUM, AND G. PEDRO SMITH^{1b}

Received December 10, 1966

The theory of ligand field splittings of $p^{2,4}$ configurations and of the relative intensities of $p^2 \leftrightarrow p^2$ electric dipole transitions has been developed and is here reported. The previously published spectrum of Bi^+ in molten salt media is rationalized very well by this theoretical model with regard to both the positions of the experimental bands and their relative intensities.

Introduction

In a recent communication we reported the preparation of Bi^+ in molten salt media and asserted that its near-infrared and visible absorption spectrum could be accounted for in terms of $6p^2 \leftrightarrow 6p^2$ intraconfigurational transitions with the $6p^2$ states perturbed by ligand fields of less than cubic symmetry.² In the present paper we shall justify this assertion by developing the ligand field theory of $p^{2,4} \leftrightarrow p^{2,4}$ electric dipole transitions and showing that it rationalizes the experimental results very well. Quite recently the ultraviolet spectrum of Bi^+ in a molten salt medium has been reported,³ and, as we shall show, these new results also are in excellent agreement with the theoretical model. It seems reasonable, therefore, to speak of bismuth(I) in the molten salt systems as having a partially filled p shell of electrons even though the exact nature of Bi^+ -ligand bonding remains unknown.

So far as we know, the only previous attempt to deal with a partially filled p shell in terms that relate to our work was a very qualitative interpretation⁴⁻⁷ of the spectrum and magnetic susceptibility of what was once believed to be I^+ with the configuration $5p^4$.

Theory

Our experimental information on Bi^+ is confined to its absorption spectra in the AlCl_3 - NaCl and ZnCl_2 - KCl eutectics as solvents and its stoichiometric formula with respect to bismuth. The data³ for the spectrum of Bi^+ in the AlCl_3 - NaCl eutectic are presented in Table I together with some theoretical quantities that will be explained later. In this table $\bar{\nu}$ denotes the wavenumber position of a band, and f denotes its oscillator strength.

In the development that follows, it is not necessary to make any specific assumptions regarding the identification of the ligands or their mode of bonding to Bi^+ . Nevertheless, in the case of Bi^+ the central bismuth atom is coordinated to something, and it seems likely that the ligands are chloroaluminate ions in the AlCl_3 - NaCl eutectic and chlorozincate ions in the ZnCl_2 - KCl eutectic. The only other possible ligands are chloride ions unattached to aluminum or zinc, but these have a very low concentration because the chloroaluminate and chlorozincate ions present are unsaturated with respect to chloride. Although we have no experimental information on coordination geometry, theoretical progress proves possible by working from general geometrical considerations.

The free Bi^+ ion has the configuration $6p^2$ with 3P_0 as ground state.⁸ Table II lists positions of intraconfigurational excited states as obtained from measurements⁹ and as calculated from the Slater-Condon-Shortly model using $F_2 = 1175 \text{ cm}^{-1}$ and $\lambda = 5840$

(1) (a) Research sponsored by the U. S. Atomic Energy Commission under contract with the Union Carbide Corp. Presented at the 22nd Annual Southwest Regional Meeting of the American Chemical Society, Albuquerque, N. M., Nov 30-Dec 2, 1966. (b) Department of Chemistry, University of Tennessee, Knoxville, Tenn.

(2) N. J. Bjerrum, C. R. Boston, G. P. Smith, and H. L. Davis, *Inorg. Nucl. Chem. Letters*, **1**, 141 (1965).

(3) N. J. Bjerrum, C. R. Boston, and G. P. Smith, *Inorg. Chem.*, **6**, 1162 (1967).

(4) J. Arotzky, H. C. Mishra, and M. C. R. Symons, *J. Chem. Soc.*, **12** (1961); J. Arotzky and M. C. R. Symons, *Quart. Rev. (London)*, **16**, 282 (1962); *Inorg. Chem.*, **2**, 880 (1963).

(5) R. F. Pasternack and T. S. Piper, *ibid.*, **2**, 429 (1963).

(6) E. E. Aynsley, N. N. Greenwood, and D. H. W. Wharmby, *J. Chem. Soc.*, 5369 (1963).

(7) R. J. Gillespie and J. B. Milne, *Inorg. Chem.*, **5**, 1577 (1966).

(8) We follow convention and use the Russell-Saunders notation to designate free-ion states even though the strong spin-orbit coupling forces in bismuth prevent S and L from being good quantum numbers (except for the 3P_1 state).

(9) C. E. Moore, National Bureau of Standards Circular 467, Vol. III, U. S. Government Printing Office, Washington, D. C., 1953, p 221.

TABLE I
BAND POSITIONS AND STRENGTHS, MEASURED AND CALCULATED^a

Measd		B ₂ ² = 0			B ₂ ² = 890 cm ⁻¹				B ₂ ² = 1780 cm ⁻¹					
10 ⁻³ ν̄, cm ⁻¹	10 ⁴ f	J _z	10 ⁻³ ν̄, cm ⁻¹	S ₁ and S ₃	10 ⁻³ ν̄, cm ⁻¹	B ₂ ² (+)		B ₂ ² (-)		10 ⁻³ ν̄, cm ⁻¹	B ₂ ² (+)		B ₂ ² (-)	
						S ₁	S ₃	S ₁	S ₃		S ₁	S ₃	S ₁	S ₃
11.1	0.7	±1	11.1	0.02	11.1	0.01	0.22 ^b	0.03	0.04	11.0	0.01	0.21 ^b	0.02	0.03
					11.2	0.04	0.05	0.01	0.33	11.3	0.05	0.07	0.02	0.23
14.4	4.5	0	14.3	0	14.3	0.03	0.01	0.03	0.01	14.1	0.07	0.03	0.07	0.03
15.2	5	±2	15.3	0.53	15.3	0.55	0.90	0.51	0.80	15.3	0.58	0.95	0.48	0.75
					15.4	0.50	0.20	0.50	0.20	15.6	0.46	0.18	0.46	0.18
17.1	37	0	17.0	0.44	17.0	0.43	0.41	0.46	0.48	17.0	0.41	0.36	0.48	0.52
		±1	17.2	0.47	17.1	0.23	0.05	0.70	0.88	17.1	0.23	0.04	0.69	0.87
					17.3	0.71	0.90	0.24	0.05	17.4	0.71	0.90	0.23	0.05
30.0	0.3	±2	30.9	0.34 ^b	30.7	0.33 ^b	0.34	0.33	0.36	30.5	0.32 ^b	0.33	0.33	0.35
					31.0	0.34	0.32	0.34	0.32	31.0	0.34	0.32	0.34	0.32
		0	31.2	0	31.5	0.32	0.33	0.31	0.32	31.8	0.32	0.33	0.32	0.33
32.5	1.5	±1	32.2	0.31	32.1	0.32	0.33	0.31	0.41	32.0	0.33	0.33	0.31	0.42
					32.4	0.47	0.41	0.32	0.33	32.6	0.31	0.41	0.32	0.33

^a The calculations used F₂ = 1056 cm⁻¹, λ = 5360 cm⁻¹, and B₀² = 8074 cm⁻¹. ^b The notation 0.32, for example, means 0.0002.

TABLE II
FREE-ION ENERGY LEVELS OF Bi⁺ FOR THE 6p² CONFIGURATION

Level	Measd, cm ⁻¹	Calcd, ^a cm ⁻¹
³ P ₀	0	0
³ P ₁	13,324	13,268
³ P ₂	17,030	17,272
¹ D ₂	33,936	33,834
¹ S ₀	44,173	44,161

^a For F₂ = 1175 cm⁻¹ and λ = 5840 cm⁻¹.

cm⁻¹. These parameters were chosen to give a best fit to the spectrum. A comparison of these energy levels with the experimental band energies in Table I shows some noteworthy similarities. In particular, ³P₀ ↔ ¹D₂ lies near the ultraviolet-band group while ³P₀ ↔ ³P₁ and ³P₀ ↔ ³P₂ lie among the near-infrared and visible bands, and ³P₀ ↔ ³P₂ almost coincides with the strongest band in the spectrum. This comparison led us to consider the possibility that the solution spectrum of the Bi⁺ complex might arise from intraconfigurational 6p² ↔ 6p² transitions split by the ligand field. We tested this idea within the approximations provided by the conventional ligand field model of intraconfigurational transitions as described below. Although this model has previously been developed in elaborate detail for d^N ↔ d^N and f^N ↔ f^N transitions, it has not, to our knowledge, been worked out in a quantitative way for p^N ↔ p^N spectra.

Our approach to the problem was the following. Using standard techniques we set up the matrix corresponding to the ligand field Hamiltonian for two electrons (or two p-electron holes, *i.e.*, electron configuration p⁴). This matrix used the entire basis set of 15 states for a p² configuration because effects due to spin-orbit coupling proved comparable to those due to the ligand field potential. If such a matrix were to apply to situations of arbitrary coordination geometry, it would contain seven undetermined parameters. These parameters would be a spin-orbit coupling constant, an electron-repulsion integral, and five parameters that describe the effect of the ligand field potential. These are too many parameters to be determined from our data. However, we found from symmetry considerations that only two potential parameters are re-

quired to describe the effects of ligand fields due to almost all of the plausible coordination geometries. Therefore, we assumed that only two potential parameters are required, and this assumption led to a matrix with four undetermined parameters.

The theory was completed by setting up equations for relative transition intensities in terms of the eigenvectors of the matrices. Obviously, relative intensities computed on the basis of the ligand field model are approximate and must be used with caution. Nevertheless, we found them to be very helpful in assigning transitions.

The final step was to vary the four parameters in the model to see how well the theory fitted the data. Values of the parameters were found that rationalized the principal features of the spectrum in a very satisfactory way.

Ligand Field States for the p² Configuration.—

The energy levels of a p² configuration within the ligand field approximation are obtained by diagonalizing the matrix corresponding to the Hamiltonian

$$H = \frac{e^2}{r_{12}} + \sum_{i=1}^2 \xi(r_i) \mathbf{s}_i \cdot \mathbf{l}_i + V \quad (1)$$

In this expression the first term describes the electrostatic repulsion between the two p electrons, the second describes their spin-orbit coupling, and the last describes the effect of a ligand field potential having the symmetry of the local static environment about the ion in question. In setting up the matrix corresponding to this Hamiltonian, we used the entire basis set of 15 states for a p² configuration and performed a simultaneous diagonalization.

The ligand field potential in eq 1 may be expressed in terms of tensor operators as

$$V = \sum_k \sum_{m=-k}^k \sum_{i=1}^2 B_m^k (C_m^{(k)})_i \quad (2)$$

where *i* is summed over the two electrons of the ion.¹⁰ Since we are dealing with p electrons, only those terms for which *k* equals 2 need be retained so that we

(10) See, for example, B. G. Wybourne, "Spectroscopic Properties of Rare Earths," Interscience Publishers, Inc., New York, N. Y., 1965.

have five potential parameters of the form B_m^2 . These five parameters describe the effect of an arbitrary ligand field on a pure p^N configuration. The fact that no other potential parameters occur signifies that the ligand field potential must have a symmetry lower than cubic in order to split the terms of a pure p^N configuration. This fact raises the possibility that the Bi^+ ion might be used to probe noncubic environments in crystals.

Examination of the properties of the symmetry point groups indicates the plausibility of a reduction in the number of potential parameters. For ligand field symmetries that belong to $C_{\infty v}$, $D_{\infty h}$, or one of the 32 crystallographic point groups other than C_1 or C_i ($=S_2$), the parameters B_{-1}^2 and B_1^2 vanish while B_{-2}^2 and B_2^2 are equal.¹¹ We neglect the C_1 and C_i point groups and suppose that the bismuth(I) complex approximates one of the remaining 32 geometries. Thus we assume that only the real parameters B_0^2 and B_2^2 are required to describe the effect of the ligand field potential to within an adequate approximation, and we write the potential in eq 2 as

$$V = \sum_{i=1}^2 \{ B_0^2 (C_0^{(2)})_i + B_2^2 [(C_2^{(2)})_i + (C_{-2}^{(2)})_i] \} \quad (3)$$

It is interesting to note that if B_0^2 is the only nonzero potential parameter, then D_{2h} , D_2 , C_{2h} , C_{2v} , and C_2 are excluded from the above list of possible point groups.

In order to calculate the matrix corresponding to the Hamiltonian in eq 1, we used the Russell-Saunders states as the basis set. These states will be designated as $|p^2SLJJ_z\rangle$. With this basis set and the ligand field potential expressed by eq 3, the matrix factors into two matrices, one of dimension 6 and the other of dimension 9. These matrices were constructed using standard tensor operator methods and the reduced matrix elements tabulated by Nielson and Koster.¹² The nonvanishing matrix elements are listed in Table III where F_2 is the Slater electron-repulsion integral, λ is the spin-orbit coupling constant (equal to half the Condon-Shortly spin-orbit coupling constant), $x = B_0^2/10$, and $y = B_2^2/(5\sqrt{2})$. The two submatrices may be constructed from this table.

Note that the matrix elements in Table III can also be used to treat the ligand field problem of the p^4 configuration by replacing λ with $-\lambda$ and leaving all other quantities unchanged.

For given values of the parameters F_2 , λ , B_0^2 , and B_2^2 , diagonalization of the matrices yields their eigenvalues, E_i , and eigenvectors, $|i\rangle$, which are the ligand field approximations to the energy levels and states of a p^2 configuration. The transition energies to be compared with the spectrum of Bi^+ are, of course, $hc\bar{\nu} = \Delta E_i = E_i - E_0$, where E_0 is the lowest eigenvalue. The ligand field states (eigenvectors) are linear combinations of Russell-Saunders states, namely

$$|i\rangle = \sum a_i (SLJJ_z) |p^2SLJJ_z\rangle \quad (4)$$

(11) See Table 5 of J. L. Prather, National Bureau of Standards Monograph 19, U. S. Government Printing Office, Washington, D. C., 1961.

(12) C. W. Nielson and G. F. Koster, "Spectroscopic Coefficients for the p^N , d^N , and f^N Configurations," Massachusetts Institute of Technology Press, Cambridge, Mass., 1963.

TABLE III
THE NONVANISHING HAMILTONIAN MATRIX ELEMENTS FOR THE
LIGAND FIELD MODEL DESCRIBED IN THE TEXT

S	L	J	J_z	S'	L'	J'	J'_z	$ p^2SLJJ_z\rangle$
1	1	1	-1	1	1	1	-1	$-5F_2 - \lambda - x$
1	1	1	-1	1	1	1	1	$-y$
1	1	1	-1	1	1	2	-1	$-3x$
1	1	1	-1	1	1	2	1	$-\sqrt{3}y$
1	1	1	1	1	1	1	1	$-5F_2 - \lambda - x$
1	1	1	1	1	1	2	-1	$\sqrt{3}y$
1	1	1	1	1	1	2	1	$3x$
1	1	2	-1	1	1	2	-1	$-5F_2 + \lambda - x$
1	1	2	-1	1	1	2	1	$\sqrt{3}y$
1	1	2	-1	0	2	2	-1	$\sqrt{2}\lambda$
1	1	2	1	1	1	2	1	$-5F_2 + \lambda - x$
1	1	2	1	0	2	2	1	$\sqrt{2}\lambda$
0	2	2	-1	0	2	2	-1	$F_2 + 2x$
0	2	2	-1	0	2	2	1	$-2\sqrt{3}y$
0	2	2	1	0	2	2	1	$F_2 + 2x$
1	1	0	0	1	1	0	0	$-5F_2 - 2\lambda$
1	1	0	0	1	1	2	-2	$2y$
1	1	0	0	1	1	2	0	$2\sqrt{2}x$
1	1	0	0	1	1	2	2	$2y$
1	1	0	0	0	0	0	0	$-2\sqrt{2}\lambda$
1	1	1	0	1	1	1	0	$-5F_2 - \lambda + 2x$
1	1	1	0	1	1	2	-2	$\sqrt{6}y$
1	1	1	0	1	1	2	2	$-\sqrt{6}y$
1	1	2	-2	1	1	2	-2	$-5F_2 + \lambda + 2x$
1	1	2	-2	1	1	2	0	$\sqrt{2}y$
1	1	2	-2	0	2	2	-2	$\sqrt{2}\lambda$
1	1	2	0	1	1	2	0	$-5F_2 + \lambda - 2x$
1	1	2	0	1	1	2	2	$\sqrt{2}y$
1	1	2	0	0	2	2	0	$\sqrt{2}\lambda$
1	1	2	2	1	1	2	2	$-5F_2 + \lambda + 2x$
1	1	2	2	0	2	2	2	$\sqrt{2}\lambda$
0	2	2	-2	0	2	2	-2	$F_2 - 4x$
0	2	2	-2	0	2	2	0	$-2\sqrt{2}y$
0	2	2	-2	0	0	0	0	$-4y$
0	2	2	0	0	2	2	0	$F_2 + 4x$
0	2	2	0	0	2	2	2	$-2\sqrt{2}y$
0	2	2	0	0	0	0	0	$-4\sqrt{2}x$
0	2	2	2	0	2	2	2	$F_2 - 4x$
0	2	2	2	0	0	0	0	$-4y$
0	0	0	0	0	0	0	0	$10F_2$

In this expression the sum is over the set of quantum numbers $SLJJ_z$. These ligand field states will be used below in an analysis of the electric dipole intensities of bands of the Bi^+ complex.

Electric Dipole Intensities.—In order to carry out an analysis of the spectrum of Bi^+ we found it necessary to use transition intensities as a guide to help in choosing between some alternative assignments. Since the observed bands had oscillator strengths on the order of 10^{-4} or greater (see Table I), we assumed the magnetic dipole and electric quadrupole mechanisms to be unimportant and computed transition intensities on the basis of the electric dipole process alone.

In order for an electric dipole transition to occur between the p^2 states, all of which have odd parity, admixing with even-parity states must occur. The most obvious source of such admixing is the absence of an inversion center in the ligand field potential due to a noncentrosymmetric arrangement of ligands, or vibrational disturbances, or some combination of these. During the past decade some aspects of the theory of these admixing mechanisms have been developed in a detailed and fairly successful way for $d^N \leftrightarrow d^N$ and $f^N \leftrightarrow f^N$ transitions. Our work was an extension of this development to the special case of $p^N \leftrightarrow p^N$ transitions. The relevant literature is too extensive to review here but we call attention to the studies of

Judd¹³ and Ofelt¹⁴ of f^N configurations, which we found especially helpful.

Electric dipole matrix elements between two Russell-Saunders p^N states will be considered first. Then linear combinations of these will be taken to obtain the matrix elements for p^N ligand field states.

The components of the electric dipole operator are

$$P_\rho^{(1)} = -e \sum_i r_i (C_\rho^{(1)})_i \quad (5)$$

where the sum with respect to i is taken over the N p -type electrons, $\rho = 0$ is the π component, and $\rho = \pm 1$ are the σ components. Matrix elements of this operator between two Russell-Saunders states, namely

$$|A\rangle = |p^N SLJ_z\rangle \quad (6a)$$

and

$$|B\rangle = |p^N S'L'J'J'_z\rangle \quad (6b)$$

vanish because of parity. However, if noncentrosymmetric interactions exist so that the ligand field potential contains odd-parity terms, V_{odd} , opposite parity states will be mixed with the pure p^N states given by eq 6. We may express the odd-parity part of the potential as

$$V_{\text{odd}} = \sum_{i(\text{odd})} \sum_{q=-l}^l \sum_i r_i^l \chi_i^q (C_q^{(l)})_i \quad (7)$$

Whether or not a particular χ_i^q term occurs and its explicit interpretation depend on details of the noncentrosymmetric interactions present in the material of interest. For example, if a particular χ_i^q occurs because of the geometry of the static environment, then $\chi_i^q = A_i^q$, where A_i^q is the standard static ligand field potential parameter. On the other hand, if the noncentrosymmetric interaction is due to small-amplitude vibrations, then $\chi_i^q = \sum_j Q_j (\partial A_i^q / \partial Q_j)$, where the Q_j

are the normal coordinates of vibration. We do not know enough about the Bi^+ complex to identify the sources of noncentrosymmetric interaction. However, even without specific information on the details of ligand geometry, we can make useful comments on electric dipole intensities based on the angular momentum properties of V_{odd} in eq 7.

Under the influence of the perturbation specified by eq 7, the states $|A\rangle$ and $|B\rangle$, given in eq 6, are mixed with opposite-parity states $|\alpha\rangle$ to become

$$|A'\rangle = |A\rangle + \sum_\alpha \frac{\langle A | V_{\text{odd}} | \alpha \rangle}{E(A) - E(\alpha)} |\alpha\rangle \quad (8a)$$

and

$$|B'\rangle = |B\rangle + \sum_\alpha \frac{\langle B | V_{\text{odd}} | \alpha \rangle}{E(B) - E(\alpha)} |\alpha\rangle \quad (8b)$$

to within first order in V_{odd} . The states $|\alpha\rangle$ are to be regarded as corresponding to the configurations $p^{N-1}l$ and $l^{4l+1}p^{N+1}$, where l has even parity, or to charge-

transfer states with the symmetry properties of l -type orbitals.

The matrix element of the electric dipole operator of eq 5 between states $|A'\rangle$ and $|B'\rangle$ yields an unwieldy expression that must be reduced by approximations before it can be applied to useful intensity considerations. We adopt the set of approximations introduced by Judd¹³ in which the energy differences in eq 8 are replaced by a single, average value ΔE_{av} . This permits the application of a closure-like procedure to the evaluation of the sum $\sum_\alpha \langle A | V_{\text{odd}} | \alpha \rangle \langle \alpha | P_\rho^{(1)} | B \rangle$ so that the tensor operators, $(C_q^{(l)})_i (C_\rho^{(1)})_j$, can be combined into a sum over single tensor operators. This leads to a simple, compact expression for the electric dipole matrix element. Discussion of the approximations involved in this procedure for the case of f^N configurations is given by Judd¹³ and Ofelt.¹⁴ These approximations should be just as valid for p^N configurations. Therefore, we take Judd's eq 13 and, applying standard tensor operator techniques, adopt it to the present situation to obtain the following approximation for the electric dipole matrix element between the states of eq 8

$$\begin{aligned} \langle A' | P_\rho^{(1)} | B' \rangle &= 5 \sum_{l,q} (-1)^{q+\rho} \chi_l^q \Xi(t, 2) \begin{pmatrix} 1 & 2 & t \\ \rho & -\rho-q & q \end{pmatrix} \times \\ &\quad \langle p^N SLJ_z | U_{q+\rho}^{(2)} | p^N S'L'J'J'_z \rangle = \\ &\quad 5 \delta_{SS'} \sum_{l,q} (-1)^{q+\rho+J+S+L+J'-J_z} \chi_l^q \Xi(t, 2) [(2J+1) \times \\ &\quad (2J'+1)]^{1/2} \begin{pmatrix} 1 & 2 & t \\ \rho & -\rho-q & q \end{pmatrix} \begin{pmatrix} J & 2 & J' \\ -J_z & q & J'_z \end{pmatrix} \left\{ \begin{matrix} J & J' & 2 \\ L & L & S \end{matrix} \right\} \times \\ &\quad \langle p^N SL || U^{(2)} || p^N SL' \rangle \quad (9) \end{aligned}$$

In this expression

$$\begin{aligned} \Xi(t, 2) &= \frac{6e}{E_{\text{av}}} \sum (2l+1) (-1)^l \begin{pmatrix} 1 & 1 & l \\ 0 & 0 & 0 \end{pmatrix} \begin{pmatrix} l & t & 1 \\ 0 & 0 & 0 \end{pmatrix} \times \\ &\quad \left\{ \begin{matrix} 1 & 2 & t \\ 1 & l & 1 \end{matrix} \right\} \langle p|r|l \rangle \langle p|r'|l \rangle \quad (10) \end{aligned}$$

where the sum is over the excited configurations connected to p^N by V_{odd} . The $\langle p|r'|l \rangle$ are radial integrals that depend on the radial functions of both the p^N and excited configurations. In eq 9, the $\langle p^N SL || U^{(2)} || p^N SL' \rangle$ are doubly reduced matrix elements which may be obtained from the tabulation of Nielson and Koster.¹²

From the properties of the $3-j$ and $6-j$ symbols that occur in eq 9 and 10, several useful observations can be made concerning the parity admixing process and the electric dipole selection rules. The original p^N -configuration states are admixed with configurations $p^{N-1}l$ and $l^{4l+1}p^{N+1}$, where l is s or d . Only those terms of V_{odd} for which l equals 1 or 3 produce parity admixing of a type which affects the electric dipole matrix element. Furthermore, the following selection rules are found to hold, namely: if S is a good quantum number, $\Delta S = 0$; if L is a good quantum number, $\Delta L \leq 2$; and if J is a good quantum number, $\Delta J \leq 2$ when $J \neq 0$ for both states of the transition, and $\Delta J = 2$ when $J = 0$ for either state of the transition. Of course, for the specific case of Bi^+ , the strong spin-

(13) B. R. Judd, *Phys. Rev.*, **127**, 750 (1962).

(14) G. S. Ofelt, *J. Chem. Phys.*, **37**, 511 (1962).

orbit coupling breaks down the above selection rules with respect to L and S . However, even though J does not remain a good quantum number in the ligand field, we find that in many situations it is almost a good quantum number so that the $\Delta J = 2$ selection rule has considerable value in the interpretation of the observed absorption spectrum. (Note that the ground state of Bi^+ in the complex is approximately $^3\text{P}_0$.)

Our primary interest is, of course, in the electric dipole matrix elements between the ligand field states of p^2 . Since these states may be expressed as linear combinations of Russell-Saunders states, the desired electric dipole matrix element, obtained from eq 9, is

$$\langle i|P_\rho^{(1)}|j\rangle = \sum_{t,q} \chi_t^q \Xi(t, 2) Y(i, j, t, q, \rho) \quad (11)$$

with

$$Y(i, j, t, q, \rho) = 5 \begin{pmatrix} 1 & 2 & t \\ \rho & -\rho - q & q \end{pmatrix} \sum_{SLJ J_z} \sum_{S'L'J' J'_z} \times \\ a_i(SLJ J_z) a_j(S'L'J' J'_z) \delta_{SS'} (-1)^{q+\rho+J+S+L+J'-J_z} \times \\ [(2J+1)(2J'+1)]^{1/2} \begin{pmatrix} J & 2 & J' \\ -J_z & \rho + q & J'_z \end{pmatrix} \begin{Bmatrix} J & J' & 2 \\ L' & L & S \end{Bmatrix} \times \\ (p^2 SL || U^{(2)} || p^2 SL') \quad (12)$$

The transition matrix element in eq 11 is related to the oscillator strength, f_ρ , of the ρ th component of the transition between states i and j through the equation¹⁵

$$f_\rho = \gamma \frac{8\pi^2 m c}{3 h c^2} \bar{\nu} |\langle i|P_\rho^{(1)}|j\rangle|^2 \quad (13)$$

In this expression γ is a term that corrects for the effect of the refractive index of the medium, and $\bar{\nu}$ is the wave-number of the transition. Experimental oscillator strengths (uncorrected for refractive index) are listed in Table I. The most significant difference between f_ρ in eq 13 and the experimental values is that the latter are averages over random orientations of the complex whereas f_ρ refers to a specific orientation. Hence, eq 13 is applied by taking a weighted sum of f_ρ over the components ρ .

If J and J_z were good quantum numbers, substantial simplifications would result both in the above sum over ρ and in $|\langle i|P_\rho^{(1)}|j\rangle|^2$. For examples of the simplifying procedures see the derivation of eq 16 and 17 in the paper by Judd¹³ and eq 6.56 in Wybourne's book.¹⁰ If J were a good quantum number and the J_z components of each J were relatively closely spaced, all oscillator strengths for the various J absorption bands of a p^N system could be related to a single parameter. In this case the theory would lead to definite quantitative predictions concerning the relative oscillator strengths of these absorption bands. However, in the case of the Bi^+ complex J and J_z are not sufficiently good quantum numbers for these simplifying procedures to be applicable so that we must examine our relations to see how far we can go toward making approximate estimates of relative intensity.

In the expression for the transition dipole matrix

(15) See, for example, L. J. F. Broer, C. J. Gorter, and J. Hoogschagen, *Physica*, **11**, 231 (1945).

element, eq 11, we can obtain numerical values of the Y functions but not of the $\chi_t^q \Xi(t, 2)$ terms. The Y functions are completely determined once values of the ligand field parameters, F_2 , λ , B_0^2 , and B_2^2 , are fixed. These parameters can be estimated by fitting transition energies, computed from the matrix of the ligand field Hamiltonian, to the observed spectra. Furthermore, there are so many $\chi_t^q \Xi(t, 2)$ terms that we cannot use them as empirical parameters. However, we do not expect the contribution of these terms to the oscillator strength to vary by any large amount from one transition to another by comparison with the very large variation in the Y functions. This expectation rests on two facts. First, the Bi^+ complexes should have completely random orientations in the liquid solution. Second, the temperature is high enough so that we reasonably suppose all relevant vibrational modes to be excited. Therefore, we shall estimate relative values of oscillator strengths from the contribution of the Y functions alone. We do not suppose these estimates to be very accurate, and we use them with caution.

Fitting the Theoretical Model to the Spectrum of Bi^+

Energy levels for the p^2 configuration were calculated for numerous values of the ligand field parameters F_2 , λ , B_0^2 , and B_2^2 . The parameters F_2 and λ were varied over ranges of $\pm 50\%$ of their free-ion values, while B_0^2 and B_2^2 were both varied over the range of $\pm 20,000 \text{ cm}^{-1}$. These calculated energy levels were compared with the measured spectrum of Bi^+ in the $\text{AlCl}_3\text{-NaCl}$ eutectic (see Table I) and several parameter sets were found which fitted the observed band positions in at least a rough way. Then relative transition intensities were estimated for these parameter sets by calculating the appropriate Y functions in eq 12. From a comparison of these estimated relative intensities with the experimental oscillator strengths we were able to discard most of these parameter sets as giving totally unsatisfactory relative intensities even when allowance was made for substantial uncertainties in the intensity estimates. These operations gave us rough estimates of the region of parameter space that best rationalized the data.

These rough estimates indicate that the near-infrared and visible bands arise from ligand field components of the free-ion $^3\text{P}_0 \rightarrow ^3\text{P}_1$ and $^3\text{P}_0 \rightarrow ^3\text{P}_2$ transitions, while the weak ultraviolet bands arise from ligand field components of the free-ion $^3\text{P}_0 \rightarrow ^1\text{D}_2$ transition.

Finally, a refined fit was made between the model and the visible and near-infrared bands to give "best" values of the ligand field parameters. This left the ultraviolet bands to serve as somewhat of a check on the fit. We found that the latter region of the spectrum was automatically rationalized quite well once the visible and near-infrared region had been fitted.

Results of computations for parameter sets close to the best fit are presented in Table I, which will be discussed in detail below. Computed relative intensity information is reported in Table I in the form of two sums of Y functions, namely

$$S_1 = \sum_{\rho} [\sum_q Y(i, j, 1, q, \rho)]^2 \quad (14a)$$

and

$$S_3 = \sum_{\rho} [\sum_q Y(i, j, 3, q, \rho)]^2 \quad (14b)$$

These sums are listed for both positive and negative values of B_2^2 . (It is not practical to list values of individual nonzero Y functions because they are so numerous.) A linear combination of S_1 and S_3 with unknown coefficients should be roughly proportional to the observed oscillator strengths. For our purpose it is sufficient to compare relative values of these sums with relative values of measured oscillator strengths.

The best fit was obtained for $|B_2^2|$ decidedly smaller than B_0^2 . Therefore, consider the special case in which B_2^2 is set equal to zero. The energy level pattern for this case is illustrated in Figure 1, and the results of calculations with best values of F_2 , λ , and B_0^2 are listed in Table I. Note that B_0^2 is positive so that we are dealing with the right-hand side of the diagram in Figure 1. For convenience we shall designate states of this diagram by giving the free-ion origin followed by the value of J_z in parentheses. Thus, on the right-hand side, ${}^3P_1(\pm 1)$ designates the first excited state. Note that the value of B_0^2 in Table I (8074 cm^{-1}) lies slightly to the left of the crossing of the ${}^3P_1(0)$ and ${}^3P_2(\pm 2)$ states. As will be seen from Table I, the parameter set $F_2 = 1056 \text{ cm}^{-1}$, $\lambda = 5360 \text{ cm}^{-1}$, $B_0^2 = 8074 \text{ cm}^{-1}$, and $B_2^2 = 0$ leads to excellent agreement between observed and computed band energies. Although ultraviolet data were not used in making the fit, the ultraviolet bands, at $30,000$ and $32,500 \text{ cm}^{-1}$, are accounted for very well in terms of the ${}^3P_0(0) \rightarrow {}^1D_2(\pm 2)$ and ${}^3P_0(0) \rightarrow {}^1D_2(\pm 1)$ transitions predicted by the model. The relative intensities of the various bands, with a single exception, are rationalized fairly well by the calculations in that the strongest bands have the greatest S_1 and S_3 values and the weakest have the smallest S_1 and S_3 values. The exception is the ${}^3P_0(0) \rightarrow {}^3P_1(0)$ band which would be completely forbidden if B_2^2 were zero but which is observed to have a significant intensity.

It is clear that if we are to account for the presence of the ${}^3P_0(0) \rightarrow {}^3P_1(0)$ transition, we must assign B_2^2 a finite value. The effect of giving B_2^2 relatively small values is presented in Table I. Note that we list results of calculations for both positive and negative values of B_2^2 . The energy values are unaffected by this sign change but S_1 and S_3 are varied somewhat, although not in a way that would provide any basis for determining which sign is correct.

For $|B_2^2|$ equals 890 cm^{-1} , the calculations show that ${}^3P_0(0) \rightarrow {}^3P_1(0)$ has a small relative intensity and five of the other transitions are split by about $100\text{--}200 \text{ cm}^{-1}$. When the value of $|B_2^2|$ is doubled to 1780 cm^{-1} , the intensity of ${}^3P_0(0) \rightarrow {}^3P_1(0)$ goes up significantly and the band splittings increase to about $300\text{--}500 \text{ cm}^{-1}$ with the largest splittings occurring in the ultraviolet region where they are least likely to be resolved because of their low intensity. Thus, as we increase $|B_2^2|$ up to

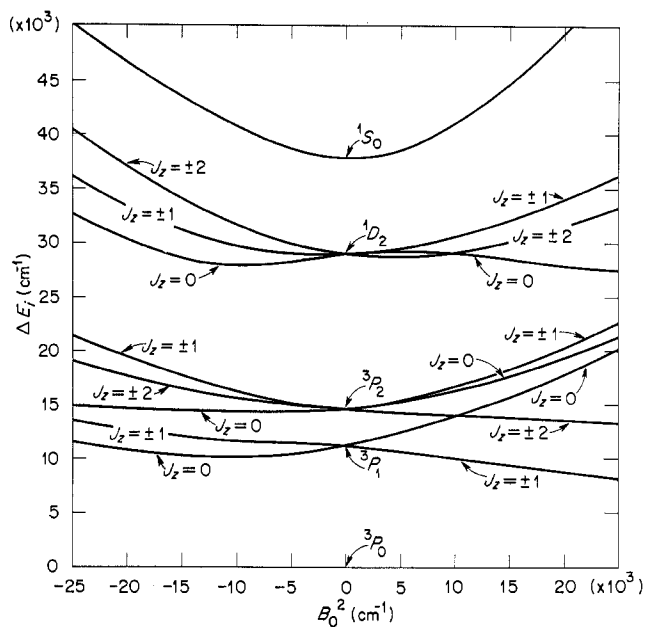


Figure 1.—Ligand field energy levels of a p^2 configuration as a function of B_0^2 with F_2 and λ fixed at 1000 and 5000 cm^{-1} , respectively. Each energy level is labeled with its J_z value, which is a good quantum number for the conditions plotted.

nearly 2000 cm^{-1} we find that the transition in question becomes weakly allowed although the S_1 and S_3 values suggest a relative intensity appreciably smaller than was observed. We do not regard this discrepancy as detracting significantly from an otherwise good fit inasmuch as S_1 and S_3 are only rough measures of relative intensity. For nonzero values of B_2^2 various bands are computed to split into two components, but for $|B_2^2|$ less than 2000 cm^{-1} the extent of splitting is too small to be observed in our spectra.

One might hope to get a better fit of the relative intensities by increasing $|B_2^2|$ significantly beyond 2000 cm^{-1} , but upon doing this, we found that the band splittings increase faster than the relative intensities improve so that this procedure is unsatisfactory.

We conclude that the best values of F_2 , λ , and B_0^2 are those listed in Table I and that $|B_2^2|$ has a relatively small but nonvanishing value. We are unable to assign a reliable value to $|B_2^2|$ but values on the order of $1000\text{--}2000 \text{ cm}^{-1}$ are probably not grossly wrong. The quality of the fit was not significantly altered by variations of $\pm 15\%$ in F_2 and B_0^2 , and of $\pm 5\%$ in λ .

It will be seen that F_2 and λ are reduced to 90 and 92% , respectively, of their free-ion values. The magnitude of this reduction is within the range found for d^N and f^N systems.

There is no satisfactory basis on which to judge the reasonableness of the B_0^2 and $|B_2^2|$ values. Nevertheless, we note that the values reported here are of the magnitude of those of B_m^k parameters required to fit some d^N and f^N systems.¹⁶ Furthermore, it is interesting that we computed B_0^2 to be positive by applying a point-charge model to a complex constructed by packing $[\text{AlCl}_4]^-$ tetrahedra about a Bi^+ ion estimated to have

(16) See, for example, values for NpF_6 in J. C. Eisenstein and M. H. L. Pryce, *Proc. Roy. Soc. (London)*, **A255**, 181 (1960).

a crystal radius of 0.98 Å. Of course one must view such point-charge estimates with much skepticism.

Returning again to Table I, it will be found that S_1 and S_3 are much lower for the ultraviolet bands than for the infrared bands whereas experiment shows these absorptions to be of more nearly comparable intensity even when generous allowance is made for experimental uncertainty. We note, however, that when account is taken of the $\bar{\nu}$ factor in eq 13 and the fact that the excited states of the ultraviolet bands are much nearer the admixed opposite-parity states than are the excited states of the infrared bands, then the discrepancy between estimated and observed relative intensities is not so large.

It was noted previously³ that under special conditions a weak shoulder is observed near 12,700 cm^{-1} , which is of uncertain origin. Let us suppose that this band belongs to the normal spectrum of the Bi^+ complex and see how this influences our theoretical analysis. What we find is that by changing F_2 , λ , and B_0^2 slightly (to 960, 5100, and 8200 cm^{-1} , respectively) and increasing $|B_2^2|$ substantially (to 5700 cm^{-1}) we can still fit the spectrum reasonably well but by no means as

well as the fit presented in Table I. The band energies deviate from the measured value by larger amounts in this fitting as compared with the previous one, and the calculated relative values of S_1 and S_3 for the 12,700- cm^{-1} band are much larger than one would expect from the measured oscillator strength. Under this new scheme the ultraviolet bands are assigned to ligand field components of the free-ion $^3P_0 \rightarrow ^1D_2$ transition, the weak infrared bands at 11,100 and 12,700 cm^{-1} are assigned to ligand field components of the free-ion $^3P_0 \rightarrow ^3P_1$ transition, while the relatively strong bands at 14,400, 15,200, and 17,100 cm^{-1} are assigned to components of the free-ion $^3P_0 \rightarrow ^3P_2$ transition. These new assignments are not greatly different from those achieved by neglecting the 12,700- cm^{-1} band.

We have not computed best parameters for the Bi^+ complex in $\text{ZnCl}_2\text{-KCl}$ but quite clearly the band assignments and even the ligand field parameters are much the same as for Bi^+ in $\text{AlCl}_3\text{-NaCl}$. Differences between the spectra of Bi^+ in these two media are attributed to differences in the ligands, presumed to be chloroaluminate ions in one case and chlorozincate ions in the other.

CONTRIBUTION FROM THE DEPARTMENT OF CHEMISTRY,
UNIVERSITY OF FLORIDA, GAINESVILLE, FLORIDA

The Chloramination of Some Substituted Stibines

BY ROBERT L. MCKENNEY AND HARRY H. SISLER

Received August 18, 1966

Triethyl-, triethyl-, tri-*n*-propyl-, tri-*n*-butyl-, and triphenylstibines react with ammonia-free chloramine or an ammonia-chloramine mixture to produce compounds of the type $[\text{R}_3\text{Sb}(\text{Cl})_2\text{NH}]$ (I). These compounds readily hydrolyze to $[\text{R}_3\text{Sb}(\text{Cl})]_2\text{O}$ (II). Further reactions of II are also described. Infrared and proton magnetic resonance studies were carried out on compounds of types I and II and on a variety of other antimony compounds. Qualitative assignments of infrared bands are given.

In earlier communications¹⁻³ it was reported that trialkylamines, trialkylphosphines, and trialkylarsines react with chloramine to produce the corresponding 1,1,1-trialkylhydrazinium, trialkylaminophosphonium, and trialkylaminoarsonium chlorides. Also, the formation of compounds of the type $\text{R}_3\text{Sb}(\text{OH})\text{Cl}$ has been reported,^{4,5} leading one to believe that the corresponding $\text{R}_3\text{Sb}(\text{NH}_2)\text{Cl}$ might be obtained by the chloramination of the trialkylstibine. However, other work⁶⁻⁹ has

shown that partial hydrolysis of trialkyl- and triaryldichlorostibanes gives the anhydride-like compounds $[\text{R}_3\text{Sb}(\text{Cl})]_2\text{O}$ and not the hydroxy chlorides. This communication describes the results of the reaction of chloramine with various trialkylstibines and triphenylstibine. The hydrolysis of these products and their reaction with either aqueous or gaseous hydrogen chloride are also described.

Experimental Section

Materials.—Tri-*n*-butyl- and triphenylstibines were purchased from M & T Chemicals, Inc. The former was redistilled and the latter was recrystallized before use. All solvents used were reagent grade and were dried and stored over calcium hydride.

The gaseous mixture of chloramine and ammonia was produced by the gas-phase reaction of excess ammonia with chlorine in a generator similar to that described by Sisler and Omietanski.¹⁰ The solution was freed of ammonia by the method of Gilson and

- (1) G. Omietanski and H. Sisler, *J. Am. Chem. Soc.*, **78**, 1211 (1956).
- (2) H. Sisler, A. Sarkis, H. Ahuja, R. Drago, and N. Smith, *ibid.*, **81**, 2982 (1959).
- (3) C. Stratton and H. Sisler, *Inorg. Chem.*, **5**, 2003 (1966).
- (4) G. Morgan, F. Mickelthwait, and G. Whitby, *J. Chem. Soc.*, **97**, 34 (1910).
- (5) H. Hartmann and G. Kuhl, *Z. Anorg. Allgem. Chem.*, **312**, 186 (1961).
- (6) A. Hantzsch and H. Hibbert, *Ber.*, **40**, 1508 (1907).
- (7) L. Kolditz, M. Gitter, and E. Rosel, *Z. Anorg. Allgem. Chem.*, **316**, 270 (1962).
- (8) G. Long, G. Doak, and L. Freedman, *J. Am. Chem. Soc.*, **86**, 209 (1964).
- (9) G. Doak, G. Long, and L. Freedman, *J. Organometal. Chem. (Amsterdam)*, **4**, 82 (1965).

- (10) H. Sisler and G. Omietanski, *Inorg. Syn.*, **5**, 91 (1957).